

AD 645233



# Technical Report

INSTITUTES FOR ENVIRONMENTAL RESEARCH IER 11-ITSA 11

## An HF Antenna Array Electronically Scanned in Elevation

R. G. FITZGERRELL

L. L. PROCTOR

A. C. WILSON

NOVEMBER, 1966

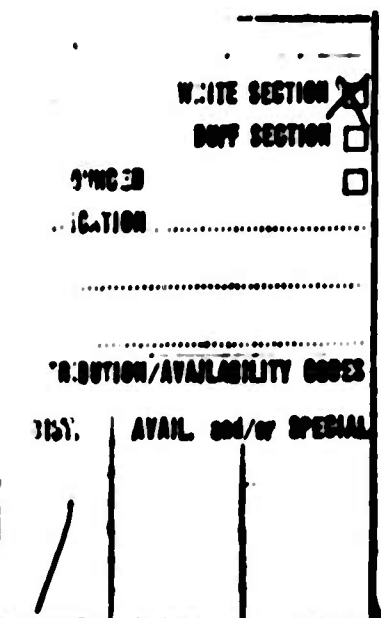
Boulder, Colorado

D D C  
REF ID: A70787  
P: 1967-181357  
FEDERAL  
CLOUDS  
B

CLEARINGHOUSE FOR FEDERAL SCIENTIFIC AND TECHNICAL INFORMATION		
Hardcopy	Microfiche	
\$3.00	\$0.65	35¢ pp
ARCHIVE COPY		

## THE INSTITUTES FOR ENVIRONMENTAL RESEARCH

The mission of the Institutes is to study the oceans, and inland waters, the lower and upper atmosphere, the space environment, and the earth, seeking the understanding needed to provide more useful services. These research Institutes are:



- **The Institute for Earth Sciences**  
conducts exploratory and applied research in geomagnetism, seismology, geodesy, and related earth sciences.
- **The Institute for Oceanography**  
works to increase knowledge and improve understanding of the ocean and its interaction with the total physical environment of the globe.
- **The Institute for Atmospheric Sciences**  
seeks the understanding of atmospheric processes and phenomena that is required to improve weather forecasts and related services and to modify and control the weather.
- **The Institute for Telecommunication Sciences and Aeronomy**  
supports the Nation's telecommunications by conducting research and providing services related to radio, infrared, and optical waves as they travel from a transmitter to a receiver. The Institute is also active in the study and prediction of periods of solar activity and ionospheric disturbance.

**Environmental Science Services Administration**

**Boulder, Colo.**



**U. S. DEPARTMENT OF COMMERCE**  
**John T. Connor, Secretary**  
**ENVIRONMENTAL SCIENCE SERVICES ADMINISTRATION**  
**Robert M. White, Administrator**  
**INSTITUTES FOR ENVIRONMENTAL RESEARCH**  
**George S. Benton, Director**

## **ESSA TECHNICAL REPORT IER 11-ITSA 11**

### **An HF Antenna Array Electronically Scanned in Elevation**

**R. G. FITZGERRELL**

**L. L. PROCTOR**

**A. C. WILSON**

**INSTITUTE FOR TELECOMMUNICATION SCIENCES AND AERONOMY  
BOULDER, COLORADO  
November, 1966**

## **FOREWORD**

**The work reported here was carried out at the request of, and supported by, Rome Air Development Center under Contract AF30(602)-2488.**

**The authors acknowledge the original contribution by Mr. H. V. Cottony of the principle of electronic scan and for general consultation on the work of the project.**

**The authors also thank Mr. C.O. Stearns and Mrs. Mary E. Chrisman for the computer programming of the antenna radiation patterns.**

**For sale by the Clearinghouse for Federal Scientific and Technical Information  
Springfield, Virginia 22151 - Price \$2.00**

## TABLE OF CONTENTS

	PAGE
<b>FOREWORD . . . . .</b>	<b>ii</b>
<b>List of Figures . . . . .</b>	<b>iv</b>
<b>Abstract . . . . .</b>	<b>1</b>
<b>1. INTRODUCTION . . . . .</b>	<b>2</b>
<b>2. SYNTHESIS OF AN ILLUMINATION FUNCTION . . . . .</b>	<b>3</b>
<b>2. 1. An Illumination Function for a Continuous Vertical Aperture . . . . .</b>	<b>3</b>
<b>2. 2. An Illumination Function for a Vertical Broadside Array of Element Antennas . . . . .</b>	<b>6</b>
<b>3. SCANNING THE VERTICAL ARRAY . . . . .</b>	<b>7</b>
<b>3. 1. Varying the Current Distribution With Respect to Time to Effect Scanning . . . . .</b>	<b>7</b>
<b>3. 2. Electronic Scan Circuitry . . . . .</b>	<b>9</b>
<b>4. ARRAY CONSTRUCTION . . . . .</b>	<b>12</b>
<b>5. RESULTS . . . . .</b>	<b>13</b>
<b>6. DISCUSSION . . . . .</b>	<b>14</b>
<b>7. CONCLUSIONS . . . . .</b>	<b>15</b>
<b>REFERENCES . . . . .</b>	<b>17</b>

## **LIST OF FIGURES**

- Figure 1.** The elevation-scan array and the adjacent azimuth-scan array.
- Figure 2.** Aperture geometry used to determine an illumination to produce a single main lobe in elevation.
- Figure 3.** Two-wave-front method of representing beam formation for an aperture with a sinusoidal current distribution.
- Figure 4.** Radiation pattern of the array as a function of elevation angle and time within a scanning cycle - 12 MHz.
- Figure 5.** Radiation pattern of the array as a function of elevation angle and time within a scanning cycle - 17 MHz.
- Figure 6.** Radiation pattern of the array as a function of elevation angle and time within a scanning cycle - 25 MHz.
- Figure 7.** Computed curve of the relationship between the sector scanned and the received frequency.
- Figure 8.** Block diagram of the electronic scanning circuits.
- Figure 9.** Block diagram of a converter unit.
- Figure 10.** Block diagram of the sideband generator.
- Figure 11.** Presentation of reception of WWV at 10 MHz showing received signals at elevation angles of  $7^\circ$  and  $32^\circ$ . Recorded at 1200 hours Dec. 6, 1962.
- Figure 12.** Presentation of the reception of WWV at 20 MHz showing a received signal at an elevation angle of  $11^\circ$ . Recorded at 1000 hours Jan. 8, 1963.

## **AN HF ANTENNA ARRAY ELECTRONICALLY SCANNED IN ELEVATION**

**R. G. FitzGerrell, L. L. Proctor, and A. C. Wilson**

### **Abstract**

An HF receiving antenna array has been constructed which is capable of electronically scanning a sector in elevation with a single, narrow, main lobe. It was incorporated into a system designed for ionospheric propagation studies which were to investigate the vertical angle-of-arrival of downcoming radio waves.

The vertical broadside array consists of ten 12-MHz to 25-MHz, horizontally polarized, log-periodic-dipole element antennas stacked with uniform spacing on a 152-m tower. The sector of scan is dependent upon the element antenna spacing, and varies with frequency. This sector is from 3° to 51.4° at 12 MHz, and is from 1.5° to 22° at 25 MHz. The half-power beamwidth of the main lobe also varies from about 7° to 3° over the same frequency range.

The main lobe of the array was scanned by varying the number of periods in the sinusoidal illumination function which was applied to the array. This scanning was effected electronically at an IF frequency, thus placing essentially no bandwidth restriction due to scanning upon the r-f input circuitry. The fundamental scan-timing frequency was 524 Hz. Each increment of the scan sector was actually scanned twice, however, once in each direction during a scanning cycle.

Photographs of the oscilloscope display are presented which show the vertical angle-of-arrival of 10-MHz and 20-MHz signals from WWV which were received at Boulder, Colorado

**Key words:** HF Vertical Array, elevation scan.

## 1. INTRODUCTION

Because of the importance of elevation angles-of-arrival in HF propagation studies, a ground-based receiving antenna array is desirable which will form a single main lobe capable of being scanned or steered in elevation. In the past, several attempts were made to construct such an array. The most noteworthy of these efforts utilized endfire phasing to obtain the desired directivity in the vertical plane. Examples of such arrays are the MUSA [Friis and Feldman, 1937], the ISCAN [Brueckmann, Gruber, and Bramble, 1962], and the MEDUSA [Morris, Mitchell, et al, 1963]. These arrays are similar in that they are capable of having their main lobes steered to the most desirable elevation angle for a particular propagation condition. The MUSA and ISCAN are linear endfire arrays while the MEDUSA is a planar endfire array which can be steered in azimuth as well as in elevation.

These endfire arrays have several disadvantages when used for HF elevation angle-of-arrival studies. They have an undesirably high degree of directivity in azimuth, and they must be many wavelengths long to achieve narrow vertical-plane beamwidths at low elevation angles. It is the low angles-of-arrival which are of primary interest in HF propagation studies.

In July 1961, work commenced on a project at the National Bureau of Standards, Boulder Laboratories, for the study of azimuthal and elevation angles-of-arrival of ionospherically propagated radio waves, both direct and backscattered, and their variations with time. A requirement of the project was to design and construct two HF receiving antenna arrays capable of being electronically scanned at a rapid rate; one scanning in azimuth, the other scanning in elevation. These arrays were to be used to observe, simultaneously though independently, the azimuthal direction and elevation angle-of-arrival of downcoming HF

radio waves. The two arrays, which were completed late 1962, are shown in figure 1.

## 2. SYNTHESIS OF AN ILLUMINATION FUNCTION

### 2.1. An Illumination Function for a Continuous Vertical Aperture

The illumination or excitation of a continuous vertical aperture which is required to generate a single main lobe in elevation can be determined using an elementary form of synthesis. The following derivation has been presented briefly by Cottony [1963] but, because this paper may not be widely available, the derivation is given in detail here. Standard antenna array theory is used to determine the illumination,  $I(h)$ , which is in general a complex variable, for a vertical aperture formed by a continuous sheet of horizontally polarized current elements. The width of this aperture,  $d_1$ , specifies the horizontal pattern factor of the individual current elements forming the aperture. For the problem at hand, this pattern factor will be assumed equal to unity since all interest during the illumination development will be directed to the vertical plane passing through the center-line of the aperture and normal to the aperture. Figure 2 depicts this geometry, and shows the location of a single current element in the aperture as well as its image in perfect ground.

The contribution of a current element in this aperture, with excitation,  $I(h)$ , to the far-zone field at an arbitrary point lying in the previously mentioned plane of interest, is given by

$$dE_n(\Delta) = \left[ I(h)e^{j\beta h} \sin \Delta - I(h)e^{-j\beta h} \sin \Delta \right] dh, \quad (1)$$

where  $h$  = the height of the current element above ground,

$\beta = 2\pi/\lambda$ ,

$\lambda$  = the signal frequency wavelength measured in the same units as  $h$ , and

$\Delta$  = elevation angle in degrees.

In this equation,  $E_n(\Delta)$  is normalized with respect to the amplitude of the field intensity due to the current element,  $dl$ , and is oriented in the direction of  $dl$ .

From (1)

$$dE(\Delta) = 2 I(h) \sin (\beta h \sin \Delta) dh, \quad (2)$$

$$E(\Delta) = 2 \int_0^H I(h) \sin (\beta h \sin \Delta) dh, \quad (3)$$

where  $E(\Delta) = E_n(\Delta)/j$ , and

$H$  = the total aperture height.

A solution for  $I(h)$  can be obtained by inspecting (3). A functional form is required for  $I(h)$  which will maximize  $E(\Delta)$  for any one specified elevation angle  $\Delta_0$ , in the range  $0 \leq \Delta \leq \frac{\pi}{2}$ . That is, when  $\Delta = \Delta_0$ ,  $E(\Delta)$  should be maximum; when  $\Delta \neq \Delta_0$ ,  $E(\Delta)$  should be as small as possible. This idea, coupled with experience gained from previous work [Cottony, 1956; Wilson, 1960], suggested the use of a sine function for  $I(h)$ . Therefore, for a specified angle,  $\Delta_0$ , let

$$I(h) = I_0 \sin (\beta h \sin \Delta_0), \quad (4)$$

where  $I_0$  is the maximum value of  $|I(h)|$ . Now using (3) and (4),

$$E(\Delta) = 2 I_0 \int_0^H \sin (\beta h \sin \Delta_0) \sin (\beta h \sin \Delta) dh, \quad (5)$$

$$= I_0 H \left\{ \frac{\sin [\beta H(\sin \Delta_0 - \sin \Delta)]}{\beta H (\sin \Delta_0 - \sin \Delta)} - \frac{\sin [\beta H(\sin \Delta_0 + \sin \Delta)]}{\beta H (\sin \Delta_0 + \sin \Delta)} \right\}, \quad (6)$$

$$= E_1(\Delta) + E_2(\Delta). \quad (7)$$

The field intensity,  $E(\Delta)$ , can be considered to consist of two components,  $E_1(\Delta)$  and  $E_2(\Delta)$ , each of which has a  $\frac{\sin x}{x}$  form. Note that the beam-width of these two components is determined by an effective aperture of

width  $2H$ , and that the amplitude of the excitation current over this effective aperture is then  $I_0/2$ . The image aperture is seen to double the effective length of the physical aperture, and to reduce the vertical beamwidth by a factor of two. It may be interesting to note that, by using the current distribution given by (4) instead of a uniform current distribution, an approximate 3 dB increase in directive gain is realized. The radiation pattern,  $|E_1(\Delta)|$ , has a  $\left|\frac{\sin x}{x}\right|$  form with the main lobe oriented at  $\Delta = \Delta_0$ . The radiation pattern,  $|E_2(\Delta)|$ , is the mirror image of  $|E_1(\Delta)|$  and has its main lobe oriented at  $\Delta = -\Delta_0$ . This lobe at  $-\Delta_0$  has no physical significance because it appears below ground level. The sidelobes of this imaginary lobe do have a physical significance because some of them may appear in the range  $0 \leq \Delta \leq \frac{\pi}{2}$ . It is the reinforcement and cancellation of the sidelobes of  $E_1(\Delta)$  and  $E_2(\Delta)$  which cause the numerous closed contours, or spots, in the contour form radiation patterns which are described later.

The current distribution given by (4) can now be rewritten as

$$I(h) = \frac{1}{2j} (I_0 e^{j\beta h} \sin \Delta_0 - I_0 e^{-j\beta h} \sin \Delta_0) \quad (8)$$

$$\text{or } I_n(h) = \frac{I_0}{2} [e^{j\beta h} \sin \Delta_0 - e^{-j\beta h} \sin \Delta_0], \quad (9)$$

where  $I_n(h) = jI(h)$ . The illumination,  $I(h)$ , can be considered as two components of equal amplitude which are opposite in sign and phase. For a specified elevation angle,  $\Delta_0$ ,  $\sin \Delta_0$  is a constant and the phase of the two components of  $I(h)$  is then a linear function of  $h$ . This means that the sine function aperture distribution may be resolved, at any specified elevation angle, into two linear distributions each having an amplitude,  $I_0/2$ . This situation is seen in figure 3 where the two components of (9) are graphically shown applied to an aperture of height,  $H$ . These two components generate the wavefronts,  $E_1(\Delta)$  and  $E_2(\Delta)$ , in the far-zone field of the aperture. The image of the physical aperture,  $OH$ ,

is  $OH'$ . The image of the positive component of  $I(h)$  is  $OW_2$ , and the image of the negative component of  $I(h)$  is  $OW'_1$ . This resolved aperture distribution produces the two main lobes as described previously -- an imaginary one in the region below ground at an angle  $-\Delta_0$  due to  $E_0(\Delta)$ , and one at  $+\Delta_0$  due to  $E_1(\Delta)$ .

## 2.2. An Illumination Function for a Vertical Broadside Array of Element Antennas

Now a transition will be made from the consideration of a continuous vertical aperture to the consideration of a vertical array of discrete, horizontally polarized, element antennas with a uniform spacing equal to twice the height of the bottom antenna above ground. The only phase distribution which will be considered corresponds to the sinusoidal distribution discussed in the preceding section.

The maximum number of periods of a sine function current distribution which can be approximated by this vertical array is  $\frac{2r - 1}{4}$ , where  $r$  is the number of the antenna counting from the bottom. This maximum occurs when each antenna is  $180^\circ$  out of phase with its adjacent antenna. Therefore, the maximum angular range of a sinusoidal current distribution applied to the array is  $\frac{\pi(2r - 1)}{2}$ .

Now rewrite (4) for the discrete array as

$$I(r) = I_r \sin \left[ \frac{\pi(2r - 1)}{2} \cdot \frac{2t}{T} \right], \quad (10)$$

where  $I(r)$  = the current distribution as a function of the antenna number,

$I_r$  = the maximum value of  $|I(r)|$ ,

$\frac{t}{T} = \frac{2h_1 \sin \Delta_0}{\lambda}$ , a dimensionless ratio which determines  $I(r)$  for a specified  $\Delta_0$ ,  $h_1$ , and  $\lambda$ ,

$\Delta_0$  = the elevation angle of the main lobe,

$h_1$  = the height of the bottom antenna above ground, and  
 $\lambda$  = the wavelength of the desired frequency of operation.

The radiation pattern for this vertical array over perfect ground, with a current distribution given by (10), can be written, by conferring with (3), as

$$|E'(\Delta)| = \left| \sum_{r=1}^n D(\Delta) I_r \sin\left[\pi(2r-1)\frac{t}{T}\right] \sin\left[\beta h_1(2r-1)\sin\Delta\right] \right|, \quad (11)$$

where  $D(\Delta)$  = the directivity of the element antenna in elevation, and  
 $n$  = the total number of element antennas in the array.

From (9), it is seen that the amplitude,  $I_0/2$ , and similarly  $I_r$ , is not a function of time or height. Therefore,  $I_r$  can be tapered to improve the main lobe versus sidelobe level -- a Chebyshev taper for instance [Dolph, 1946]. This taper is applied with the maximum amplitude at the bottom (or number one antenna) tapering to a minimum at the top antenna. The taper is applied in this manner because the image forms one-half of the effective aperture for which the taper is calculated.

### 3. SCANNING THE VERTICAL ARRAY

#### 3.1. Varying the Current Distribution With Respect to Time to Effect Scanning

In section 2.1, it was shown that the sinusoidal current distribution, at any specified elevation angle,  $\Delta_0$ , could be considered as the superposition of two linear distributions. So, to scan this array,  $\sin\Delta_0$  is made to increase linearly with respect to time. An examination of (8) shows that the phase of  $I(h)$ , and similarly the phase of  $I(r)$ , will then increase linearly with respect to time at any value of  $h$  or chosen antenna location,  $(2r-1)h_1$ . The linear function of time which is chosen to replace  $\sin\Delta_0$  is

$$\sin\Delta_0 = \frac{\lambda t}{2h_1 T}, \quad (12)$$

where  $T$  = the scanning period in seconds, and  
 $t$  = time in seconds.

This replacement of  $\sin \Delta_0$  is necessary because the main lobe passes into the imaginary region for  $\sin \Delta_0 > 1$ . The grating lobes are relied upon to provide an infinite supply of new lobes as the old ones pass out of the sector  $0 \leq \Delta \leq \frac{\pi}{2}$ . These grating lobes appear at the angles

$$\Delta_G = \sin^{-1} \left[ \frac{(2n - 1)\pi}{2\beta h_1} \right], \quad n = 2, 3, 4 \dots \quad (13)$$

$$= \sin^{-1} \left[ \frac{(2n - 1)\lambda}{4h_1} \right], \quad n = 2, 3, 4 \dots \quad (14)$$

on either side of the two contra-rotating main lobes. The main lobe of interest in any scanning period beyond the first one, can be located using

$$\Delta'_0 = \sin^{-1} \left[ \frac{\lambda}{2h_1} \left( \frac{t}{T} - \frac{n}{2} \right) \right], \quad (15)$$

where  $n$  is an integer chosen so

$$0 \leq \left( \frac{t}{T} - \frac{n}{2} \right) \leq 1. \quad (16)$$

Now returning to figure 3, as  $\frac{t}{T}$  increases the lobe formed by the effective aperture illumination,  $W_2 W'_1$ , rotates counterclockwise from  $+\Delta_0$  toward  $\frac{\pi}{2}$ . At the same time, the imaginary lobe formed by  $W_1 W'_2$  rotates clockwise from  $-\Delta_0$  toward  $-\frac{\pi}{2}$ . That is, the main lobe is moving up as the imaginary lobe moves down prior to the time the grating lobe adjacent to the main lobe appears at  $\frac{\pi}{2}$  (providing  $h_1 = \frac{\lambda}{4}$ ). In this situation,  $\sin \Delta_0$  is approaching +1 and  $\frac{t}{T}$  is approaching 0.5.

This description of the main lobe position corresponds to  $0 < \frac{t}{T} < 0.5$  in the contour-form radiation patterns given in figures 4, 5, and 6. These patterns were computed using (11) and show  $|E'(\Delta)|$  as a function of  $\Delta$  and  $\frac{t}{T}$  for the ten-element array of log-periodic dipole

antennas situated over perfect ground. Also included in the computation was the application of a Chebyshev current distribution to  $I_r$ . This limited the sidelobes of  $|E'(\Delta)|$  to a level 30 dB below the main lobe.

As previously shown, the angular spacing between the main lobe and the first grating lobe, and between all successive grating lobes, is equal to  $\sin^{-1}(\frac{\lambda}{4h_1})$ . If  $\sin^{-1}(\frac{\lambda}{4h_1}) > \frac{\pi}{2}$ , there will be a portion of the scanning period in which no main lobe is present in the sector  $0 \leq \Delta \leq \frac{\pi}{2}$ . If  $\sin^{-1}(\frac{\lambda}{4h_1}) < \frac{\pi}{2}$ , there will be a portion of the scanning period when more than one main lobe is present in this sector. The latter situation occurs for the array described herein as seen in figures 4, 5, and 6. As a result, the vertical array has a primary sector of scan determined by the electrical separation of the element antennas. A computed curve showing the relationship between the maximum elevation angle of the primary sector and the received signal frequency is shown in figure 7.

### 3.2. Electronic Scan Circuitry

In the offset-frequency scanning technique [Cottony and Wilson, 1961] used to scan the main lobe of the array described here,  $\sin \Delta_0$  is made to increase linearly with time in the electronic circuitry of the scanning system. The resulting phase variation of  $I(r)$  can be introduced in converters of the receiving system which are connected to each individual antenna of the array. The function of the converter is to modulate the signal received by its associated antenna with two current distributions of opposite polarity with equal, but opposite, phase displacements. For a receiving system, this can be accomplished by modulating the received signal voltage,  $e_0 \sin \omega_0 t$ , with two heterodyne voltages having this prescribed relationship.

For the  $r$ th converter these voltages will be

$$e_{rl} = e_0 \sin [\omega_0 t + (2r - 1)\phi], \quad (17)$$

$$e_{r2} = -e_0 \sin [\omega_0 t - (2r - 1)\phi]. \quad (18)$$

For a scanning antenna,  $\phi$  is a function of time and will be denoted as  $\omega_s t$  where  $\omega_s$ , the angular frequency of scan, is  $2\pi$  times the scan rate. This gives

$$e_{sr1} = e_0 \sin [\omega_0 + (2r - 1)\omega_s]t, \quad (19)$$

$$e_{sr2} = -e_0 \sin [\omega_0 - (2r - 1)\omega_s]t. \quad (20)$$

These two voltages are functions of the same variable,  $t$ , and are, therefore, coherent signals. Combining (19) and (20) yields

$$e_{sr1} + e_{sr2} = 2e_0 \cos \omega_0 t \sin (2r - 1)\omega_s t$$

or

$$\frac{1}{2}(e_{sr1} + e_{sr2}) = e_0 \cos \omega_0 t [1 + \sin (2r - 1)\omega_s t] - e_0 \cos \omega_0 t. \quad (21)$$

The sum of the two desired heterodyne voltages is seen to be equal to the basic, or center frequency, heterodyne voltage modulated by a voltage with a frequency equal to  $(2r - 1)$  times the angular frequency of scan, with the fundamental suppressed. This, in effect, describes the manner in which the heterodyne voltages were generated. A set of coherent phase-locked voltages, with frequencies equal to odd multiples of  $\omega_s$ , were generated. These modulated the fundamental sideband-generator voltage, and each pair of sidebands was delivered to a converter while the fundamental was suppressed.

It should be noted here that the amplitude of the heterodyne voltage varied sinusoidally, so the output of the converters was a linear function of the incoming signal and the heterodyne voltages.

The relationship between the various components of the electronic circuitry is shown in the block diagram in figure 8. The electronic circuit and mechanical component arrangement of the units comprising

the vertical scan system were designed so that all variable tuning capacitors could be driven from a single shaft through speed reducers. In this manner, the operating frequency of the system could be changed rapidly. The tracking was adequate for coarse tuning; however, to obtain minimal sidelobe levels, each unit was adjusted separately at the desired frequency.

The converter units, as seen in figure 9, consisted of four separate stages: a 12- to 25-MHz tuned-input tuned-output preamplifier stage; a first mixer with 455-kHz output coupled into the second mixer stage by means of a single-tuned transformer giving a half-power bandwidth of approximately 6 kHz; a second mixer; and finally, an isolation amplifier with a gain control which amplified and set the level of the sideband-generator signal to the second mixer. This gain control set the output level of each unit so that a Chebyshev distribution was obtained. This gave the narrowest possible beamwidth for the desired sidelobe level.

The sideband generator, see figure 10, provided a set of phase-locked frequencies to the converter units which were 1.3 MHz plus and minus  $(2r - 1) (524 \text{ Hz})$ , for  $r = 1$  to 10. That is, unit number one, the unit receiving its input signal from the bottom or number one antenna, received a pair of phase-locked frequencies for its second mixer which were 1.300524 MHz and 1.299476 MHz; unit number two received 1.301572 MHz and 1.298428 MHz; etc. These phase-locked frequencies were obtained as follows: a 524-Hz tuning fork frequency standard was used to generate 524 Hz, 1572 Hz, 2620 Hz, . . . , 9956 Hz, by one doubling and nine subsequent mixing operations. Next, these phase-locked audio signals were delivered through separate phase-adjusting networks to ten balanced-modulator circuits where they were mixed with a 1.3-MHz carrier signal from a crystal-controlled oscillator. Finally, the sideband pairs at the output of each balanced modulator were delivered through cathode followers to the converter units.

The 1.755-MHz amplifier-detector unit consisted of a tuned-input tuned-output preamplifier followed by two wide-band amplifiers and a detector. The input circuit parameters set the half-power bandwidth for the entire unit at about 20 kHz. An emitter follower was provided to supply an undetected 1.755-MHz signal for tuning purposes, while the detected output was delivered to the oscilloscope for display.

The receiver bandwidth requirement of any scanning array will be greater than the minimum bandwidth of the same array with a fixed beam. The bandwidth of the vertical-scan system was determined only by the r-f input circuitry of the converters, since scanning was accomplished at the IF frequency. This placed a 20-kHz bandwidth requirement on the second mixer and all of the circuitry that followed -- not on the converter r-f input.

To preserve the phase relationships of the received signals, the coaxial cables between each antenna and its converter were electrically equal in length, as were all signal cables performing identical functions within the system.

#### 4. ARRAY CONSTRUCTION

The work of designing and constructing the azimuth-scan array was completed in May 1962, and was reported in RADC Report No. RADC-TDR-62-549 [Tveten, et al., 1962]. The construction of the vertical array was started May 1962, and was completed in December 1962. Both arrays are located at the Institute for Telecommunication Sciences and Aeronomy Table Mountain field site, north of Boulder, Colorado. The vertical array is positioned at the south end of the azimuth-scan array, and consists of 10 log-periodic-dipole element antennas mounted on a 152-m tower. These element antennas are uniformly spaced 16 m apart, as shown in figure 1, with the bottom antenna 8 m above the ground. The phase centers of the element antennas

of both arrays form a vertical plane oriented normal to a line bearing 114° East of true North.

The element antennas used for this array are identical to those used in the azimuth-scan array except for the method of mounting them on the tower. The VSWR of each element antenna is less than 2:1 over the frequency range of 12 MHz to 25 MHz. The gain of each element antenna is about 7 dB above isotropic, and the minimum front to back ratio is about 20 dB. The E and H-plane half-power beamwidths are  $75^\circ \pm 10^\circ$  and  $115^\circ \pm 10^\circ$  respectively.

## 5. RESULTS

The 1.755-MHz output signal of the scanning system was cyclic at a 524-Hz repetition rate and was viewed on an oscilloscope using an A-scan type of display. The oscilloscope's horizontal sweep was triggered by the 524-Hz tuning fork frequency standard and the detected output of the 1.755-MHz amplifier-detector unit was connected to the oscilloscope's vertical amplifier input. This arrangement displayed the signal amplitude as the ordinate and the sine of the elevation angle of arrival as the abscissa. Since the abscissa was actually calibrated in degrees of elevation angle, this scale was not linear.

Figures 11 and 12 are photographs of the display of signals received at Boulder from WWV. The photographs were rotated 90° clockwise to aid in their interpretation. The left-hand trace shows signal amplitude versus elevation angle. The right-hand trace is a simulated antenna array pattern obtained by applying equal amplitude calibration signals, alternating 180° in phase, to the converters. The converter of the bottom antenna received a positive signal, the next antenna received a negative signal, etc. This calibration simulated a signal arriving at the point of reinforcement of the two main beams which

sweep the sector. Thus, the simulated pattern permitted calibration of the elevation angle-of-arrival scale on this photograph.

## 6. DISCUSSION

In the Introduction section of this paper, it was stated that the endfire type of array had several disadvantages when compared to the vertical broadside array illuminated with a sinusoidal current distribution. To be specific, calculations were made which determined the length required of a free-space endfire array of isotropic elements, spaced 16 m apart, to produce a main lobe with a half-power beamwidth in the vertical plane equal to that produced by a ten-element vertical array, over perfect ground, of isotropic elements spaced 16 m apart. At a signal frequency of 17 MHz, with the main lobe of each array oriented 10° above the horizontal, the beamwidth was 2.8°. The vertical array was 152 m high while the endfire array was 1520 m long. The endfire array must be even longer, of course, to equal the beamwidth produced by the vertical array at elevation angles less than 10° above horizontal.

As stated in section 4, the phase centers of the azimuth-scan and vertical-scan arrays form a vertical plane. A Mills Tee could be formed if the two arrays were operated as a unit. To facilitate operation in this manner, the scanning rate of the vertical array was set at 524 scans per second and the scanning rate of the azimuthal array was set at 500 scans per second. The common sector lying in front of the plane of the antennas could then be scanned 24 times in one second. This overall scan rate was to allow convenient recording of data on film using a camera operating 24 frames per second. A Mills type of antenna will give ambiguous direction-of-arrival

information for frequency coherent signals arriving from different directions. This is a characteristic of multiplicative arrays for which the output is the product of the outputs of two separate linear arrays.

The original experimental circuitry, which demonstrated the feasibility of the scanning technique, is no longer in operation. This is partly a result of unexpected image rejection requirements encountered in the reception of ionospheric backscatter signals. As a result, the system is now in a state of conversion to a steerable system using different circuitry.

The recorded output of the array shown in figures 11 and 12 gives the elevation angles of 10 MHz and 20 MHz signals received from WWV. These signals appear at about  $7^\circ$  and  $32^\circ$  in figure 11, and about  $11^\circ$  in figure 12. The response at about  $69^\circ$  in figure 11 can be ignored because it occurs at the point of reinforcement of the two main beams where the array gain is about 6 dB higher than it is in the remainder of the sector shown in this figure.

Regrettably, the time and financial conditions immediately following the completion of the vertical array did not permit extensive operational tests to be performed by the authors. A new array design such as the one described here deserves full-scale testing preferably by flying an aircraft borne transmitter in the far-field of the array. The performance of the array could then be checked by comparing the elevation angle data from the array with optical or radar tracking information from the aircraft.

## 7. CONCLUSIONS

A vertical broadside array of uniformly spaced element antennas, illuminated with a sinusoidal current distribution, has been shown to produce a single main lobe in elevation which can be scanned at rapid rates.

The completed work also indicated that the scanning technique, described herein, is practical and can be instrumented with fairly simple electronic circuitry.

## REFERENCES

1. Brueckmann, H., J. Gruber, and C. Bramble (1962), ISCAN -- Inertialess steerable communication antenna, 1962 IRE International Con. Rec., Pt. 1, pp. 152-163.
2. Cottony, H. V. (1956), High gain antennas for VHF scatter propagation, IRE Trans. on Comm. Systems, Vol. CS-4, No. 1, pp. 56-63.
3. Cottony, H. V., and A. C. Wilson (1961), A high-resolution rapid scan antenna, NBS J. Res. (Radio Prop.) 65 D, No. 1, pp. 101-110.
4. Cottony, H. V. (1963), Current development in an electronically scanned antenna, Symposium on Electromagnetic Theory and Antennas, Copenhagen, June 25-30, 1962, (Pergamon Press).
5. Dolph, C. L. (1946), A current distribution for broadside arrays which optimizes the relationship between beamwidth and side-lobe level, Proc. IRE, Vol. 34, pp. 335-348.
6. Friis, H. T., and C. B. Feldman (1937), A multiple unit steerable antenna for short wave reception, BSTJ, Vol. 16, No. 3, pp. 337-419.
7. Morris, D. W., G. Mitchell, and others (1963), An experimental multiple-direction universally-steerable aerial system for HF reception, Proc. IEE, Vol. 110, No. 9, pp. 1569-1582.
8. Tveten, L. H., D. R. Macken, A. C. Wilson, R. G. FitzGerrall, J. E. Adams, and L. L. Proctor (1962), High frequency propagation back-scatter and phase studies, RADC Rept. No. RADC-TDR-62-549.
9. Wilson, A. C. (1960), Oblique incidence receiving antenna array for a relative ionospheric opacity meter, NBS Tech. Note No. 78.

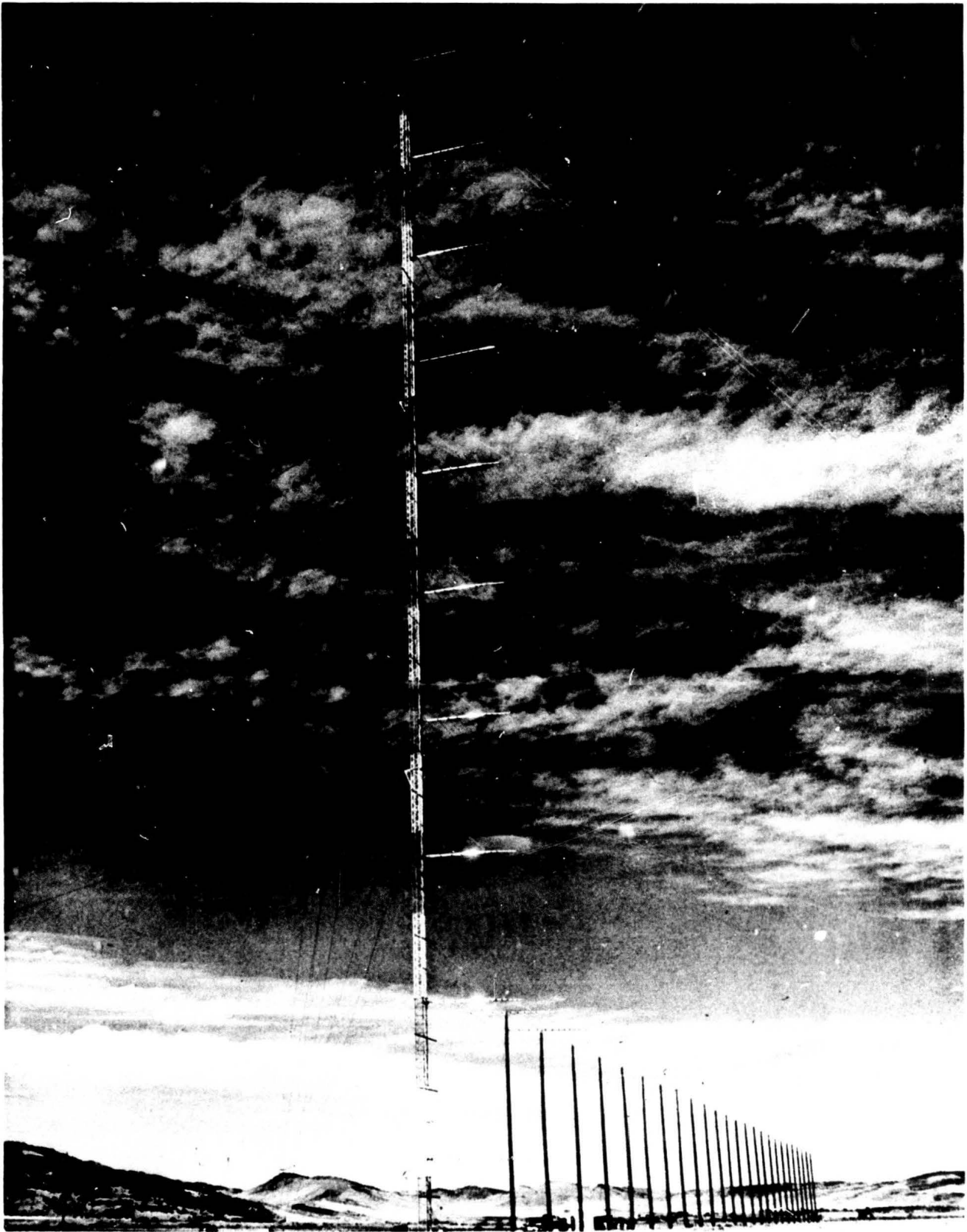


Figure 1 The elevation-scan array and the adjacent azimuth-scan array.

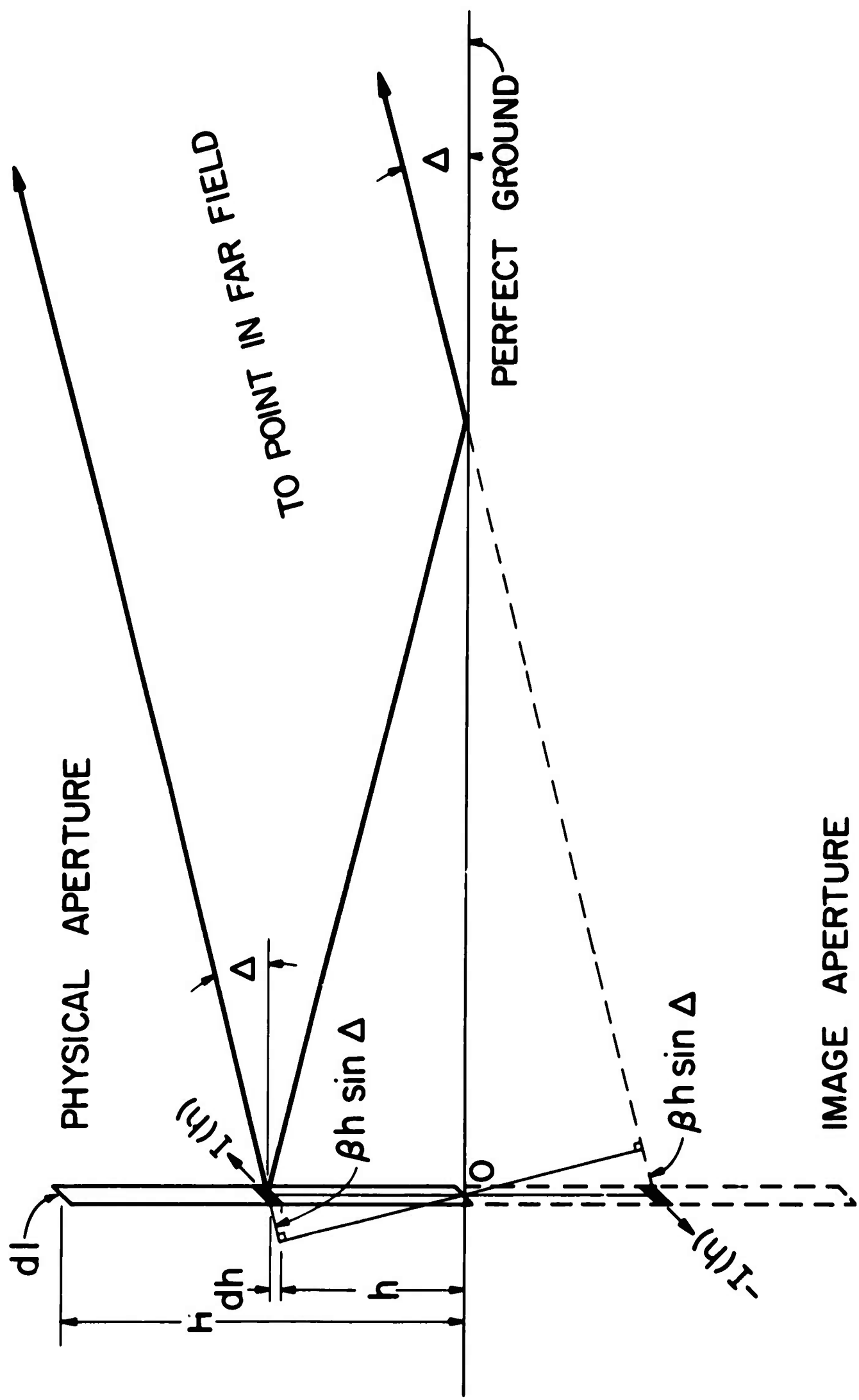


Figure 2 Aperture geometry used to determine an illumination to produce a single main lobe in elevation.

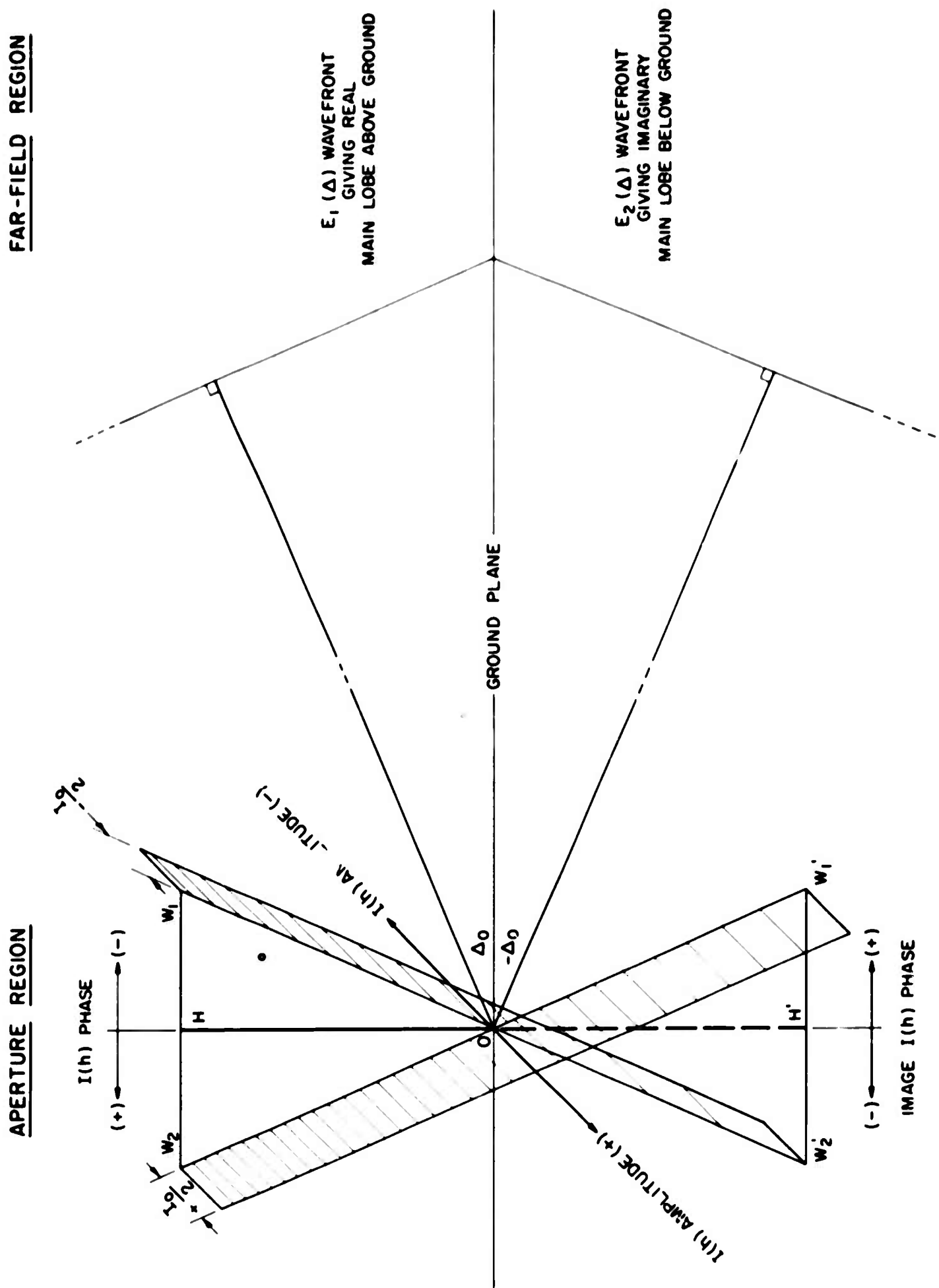


Figure 3 Two-wave-front method of representing beam formation for an aperture with a sinusoidal current distribution.

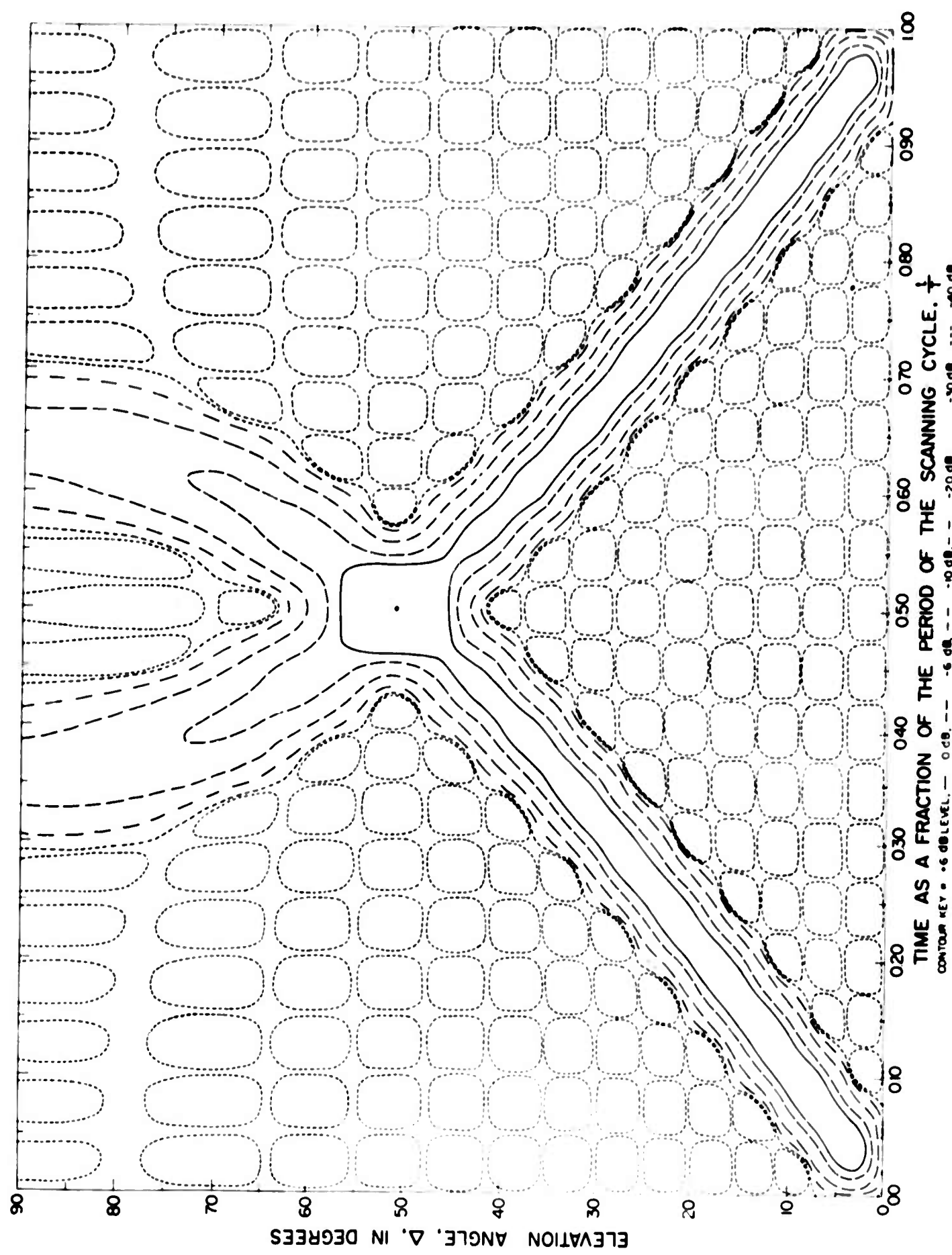


Figure 4 Radiation pattern of the array as a function of elevation angle and time within scanning cycle - 12 MHz.

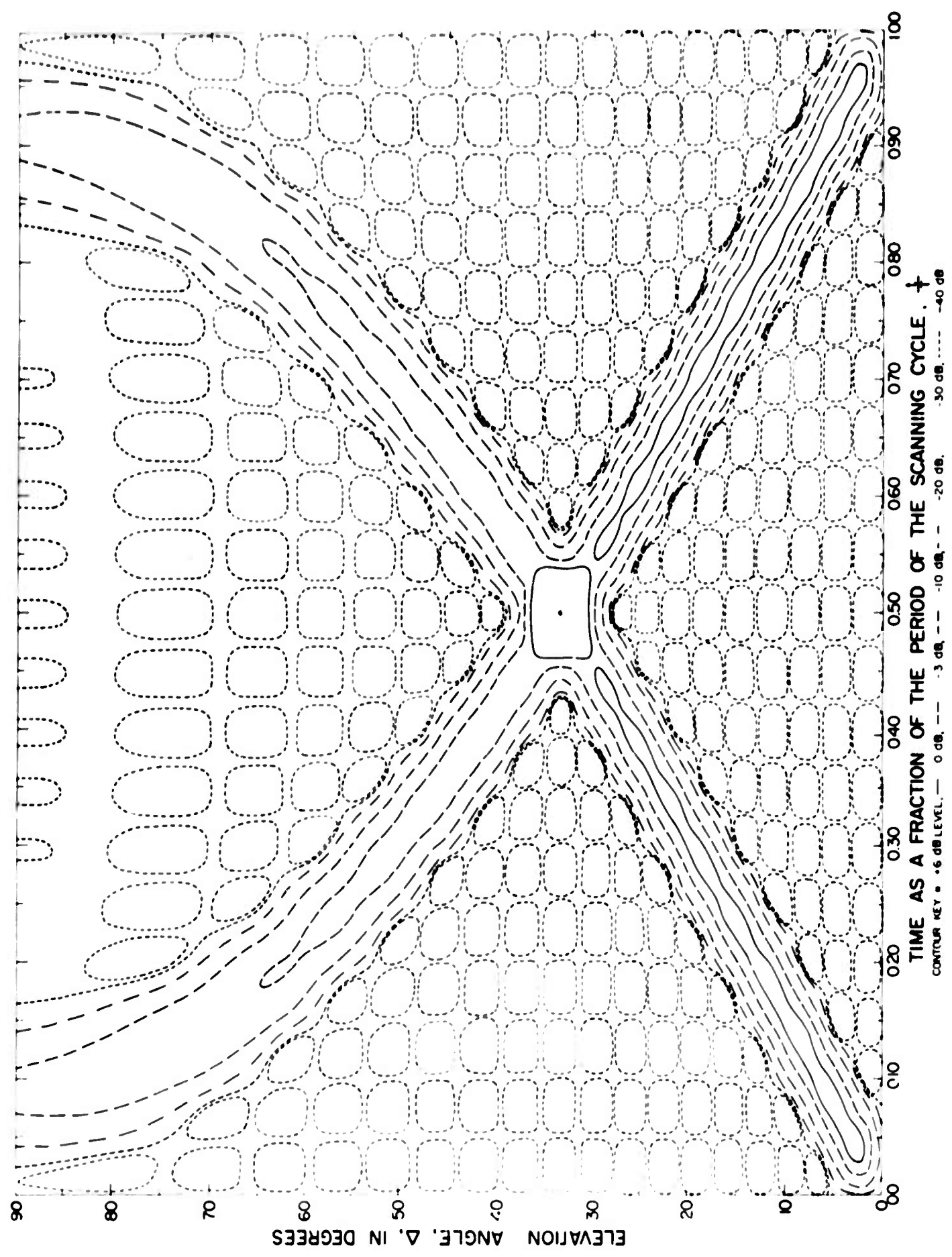
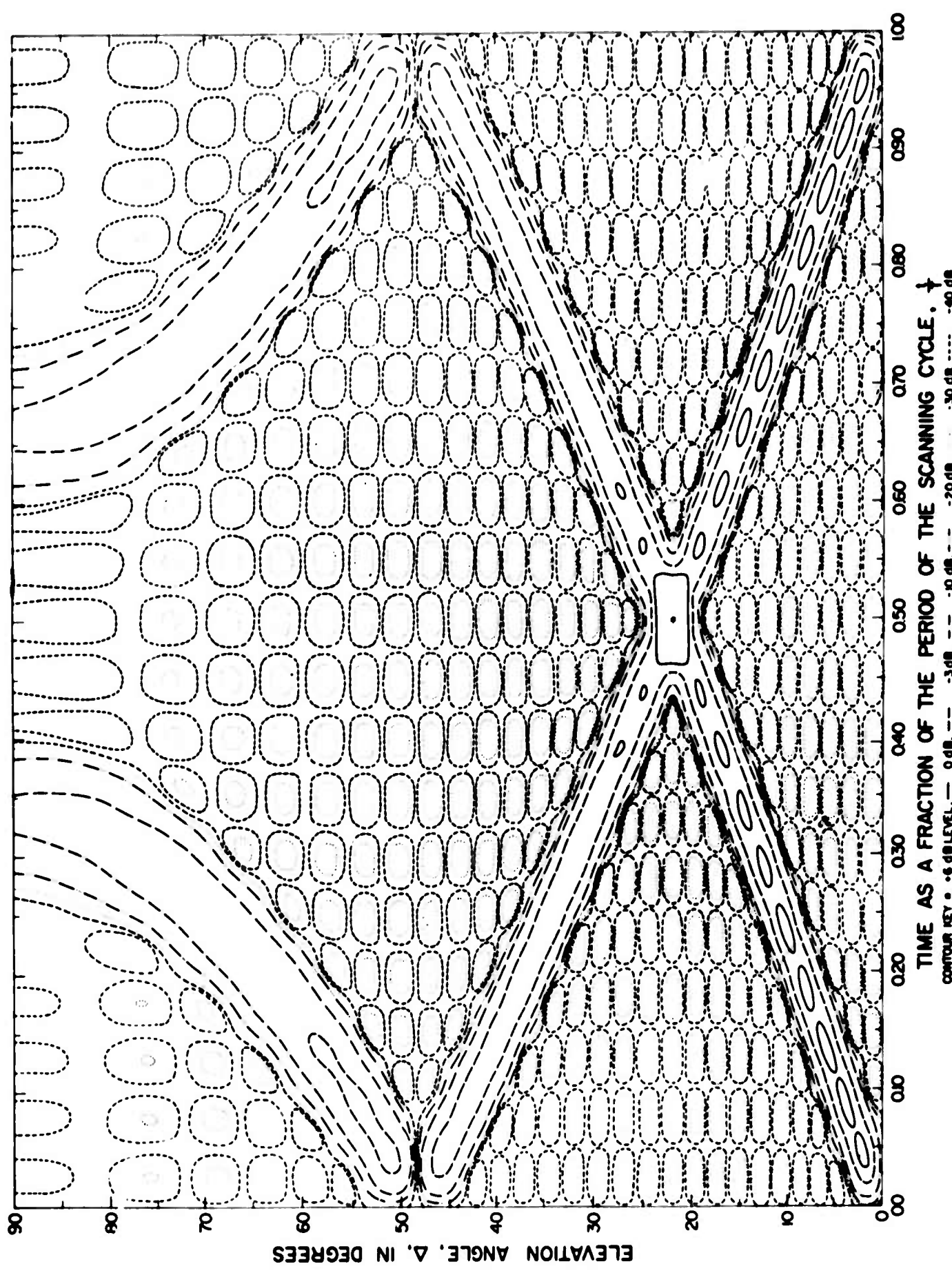


Figure 5 Radiation pattern of the array as a function of elevation angle and time within a scanning cycle -- 17 MHz.



**Figure 6** Radiation pattern of the array as a function of elevation angle and time within a scanning cycle -- 25 MHz.

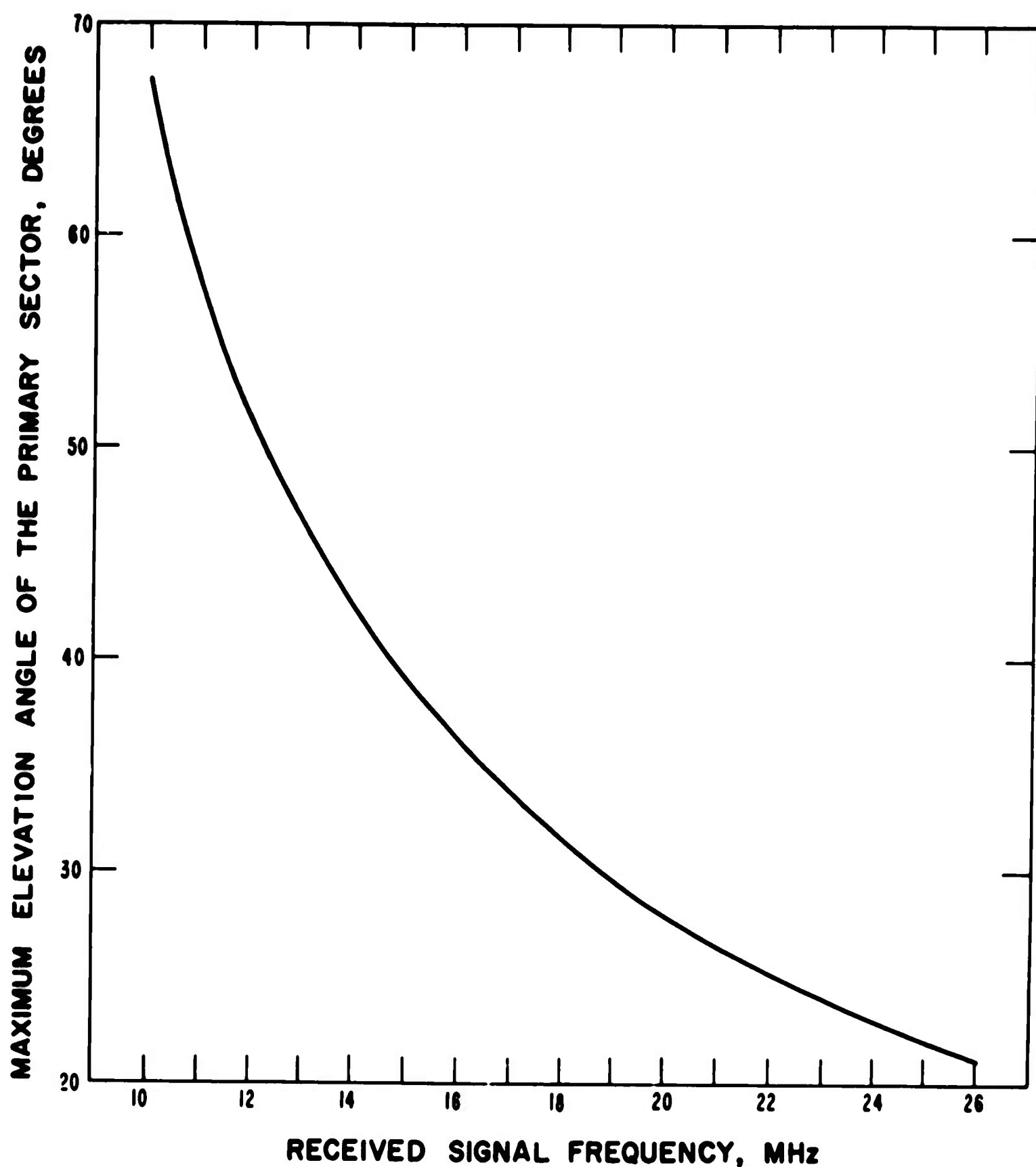


Figure 7 Computed curve of the relationship between the sector scanned and the received frequency.

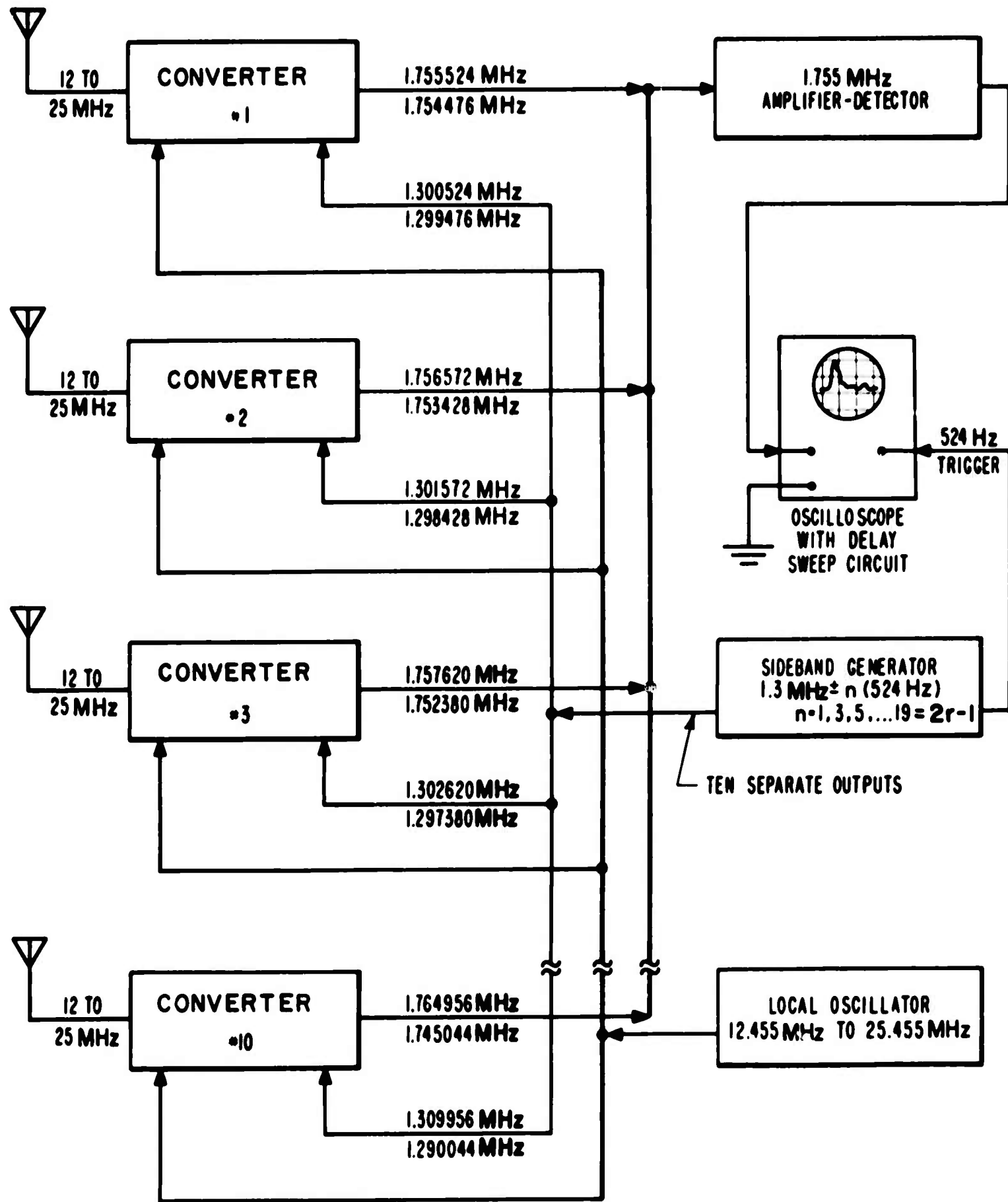


Figure 8 Block diagram of the electronic scanning circuits.

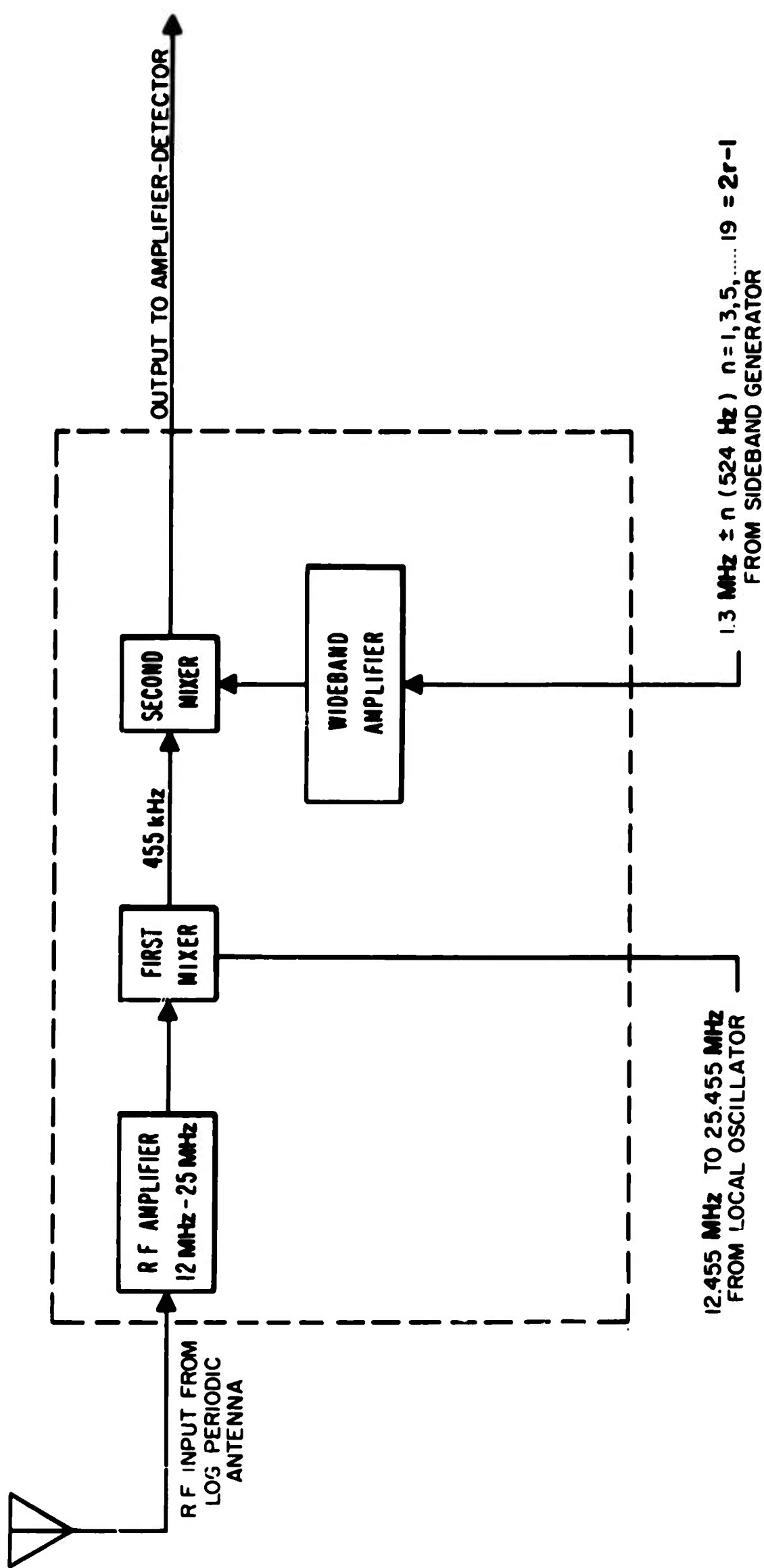


Figure 9 Block diagram of a converter unit.

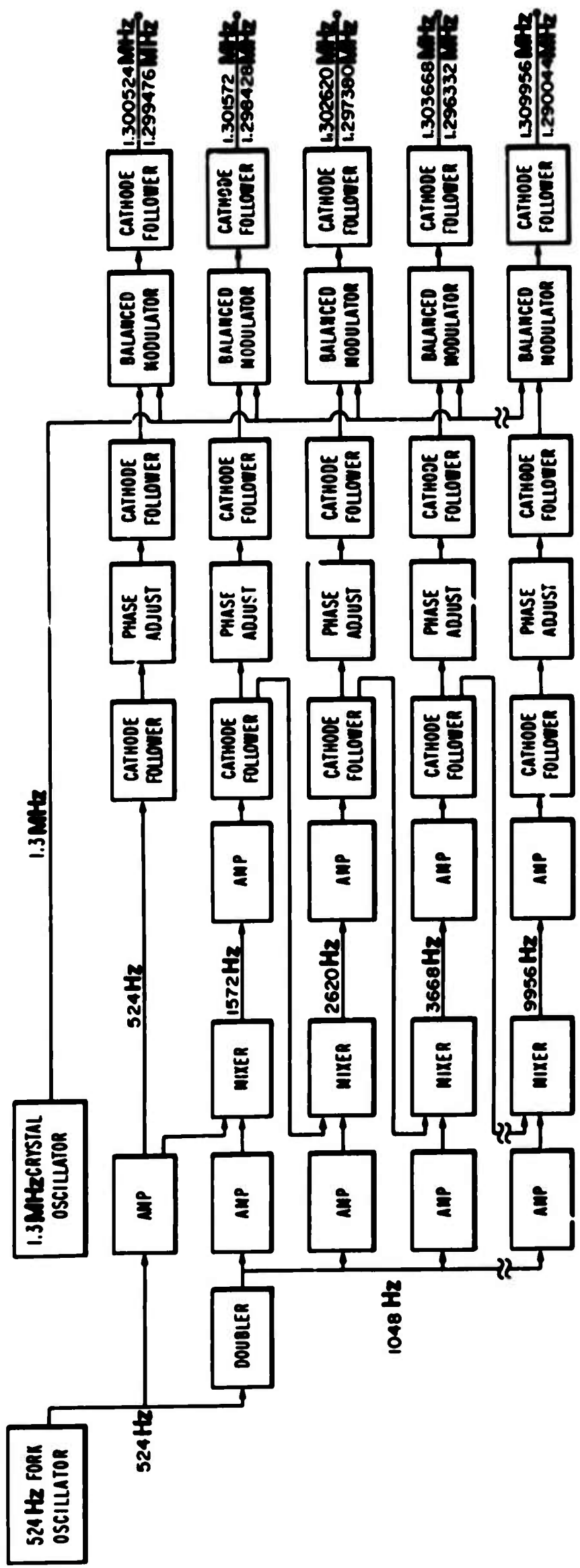


Figure 10 Block diagram of the sideband generator.

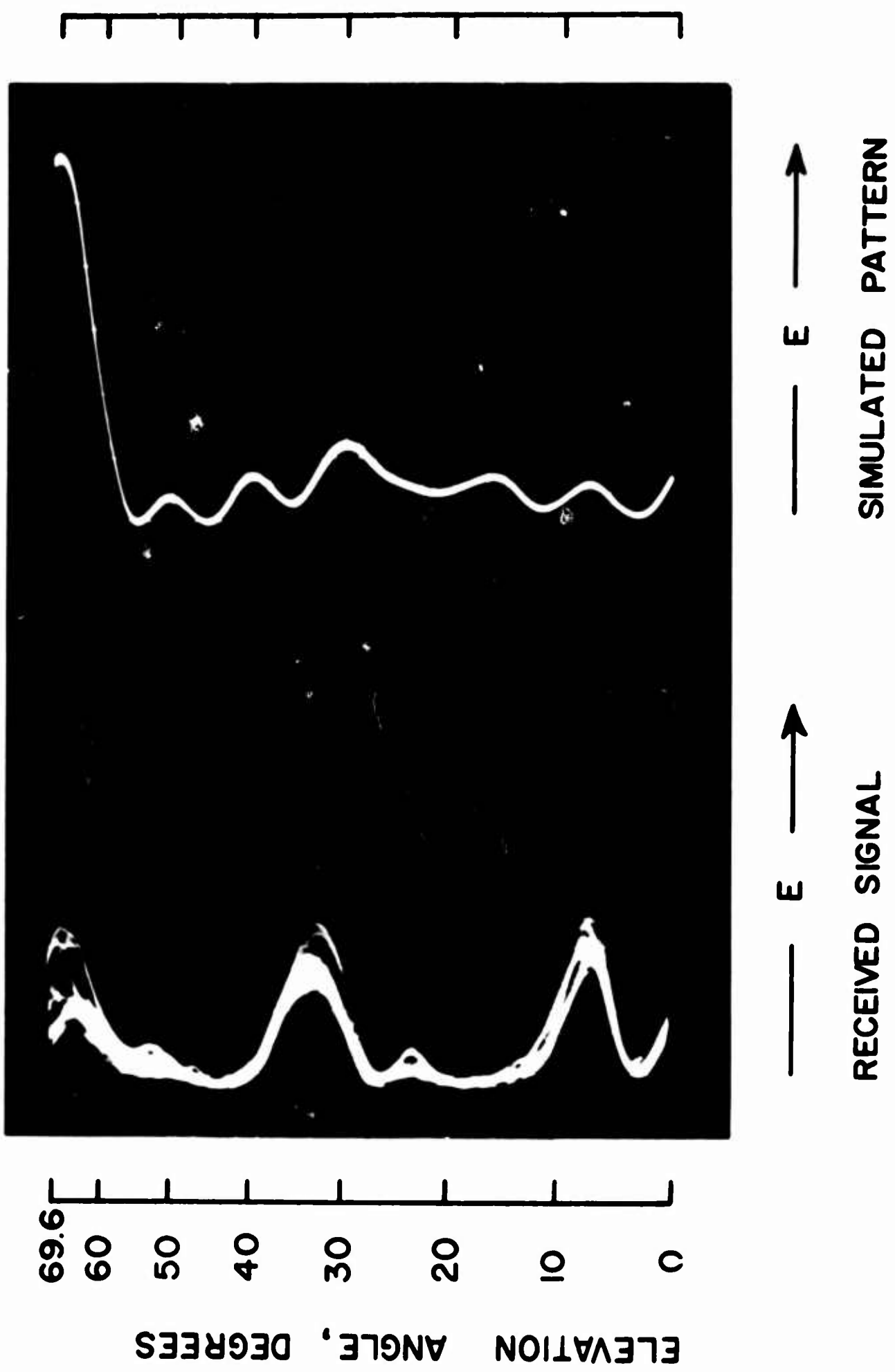


Figure 11 Presentation of the reception of WWV at 10 MHz showing received signals at elevation angles of  $7^{\circ}$  and  $32^{\circ}$ . Recorded at 1200 hours Dec. 6, 1962.

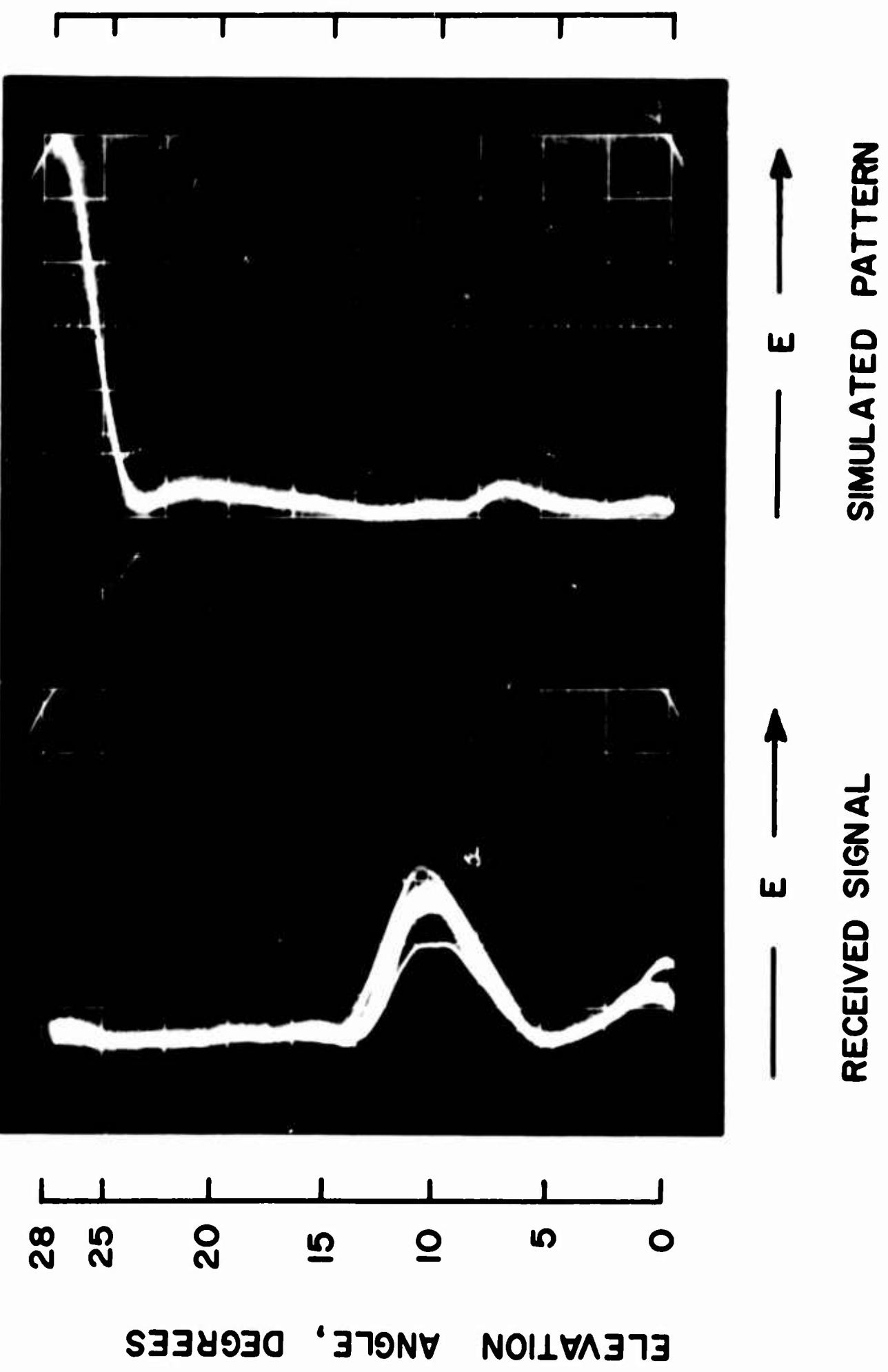


Figure 12 Presentation of the reception of WWV at 20 MHz showing a received signal at an elevation angle of  $11^\circ$ . Recorded at 1000 hours Jan. 8, 1963.